Emulating 3D-Var data assimilation using autoencoder-like methods

Boštjan Melinc[1], Žiga Zaplotnik[2,1]

[1]University of Ljubljana, Faculty of Mathematics and Physics
[2]European Centre for Medium-Range Weather Forecasts

Contents

- Motivation
- Method
  - Design of variational autoencoder (VAE)
  - 3D-Var cost function in the latent space of a VAE
  - Background-error covariance modelling
- Single observation experiments
  - univariate case (T_{850})
  - multivariate case (Z_{200}, u_{200}, v_{200})
- Alternative to using VAE: probabilistic autoencoder (PAE)
- Conclusions and outlook

Motivation

- Variational data assimilation: find the **most likely state** of the atmosphere given the *previous forecast (background)* and *new observations*
  - 3D-Var: all observations valid at *the same time*
  - 4D-Var: observations valid at *different times*
- 3D/4D-Var in global numerical weather prediction (NWP) models **too expensive** to be performed in **gridpoint space** => it is performed in a **control space** defined by analytical transformations utilising manually-defined physical balances and correlations
- Weakness: **tropical balances are not adequately represented** using these analytical transformations
- **Idea: Use neural-network-discovered transformations** from gridpoint space to a reduced-order latent space and perform variational cost function minimisation in the latent space

Variational autoencoder (VAE)

- VAE architecture based on Brohan (2022)
- Input data: daily mean T_{850} from ERA5 reanalysis on latitude-longitude grid (0.25˚ × 0.25˚ resolution → 720 × 1440 grid points)

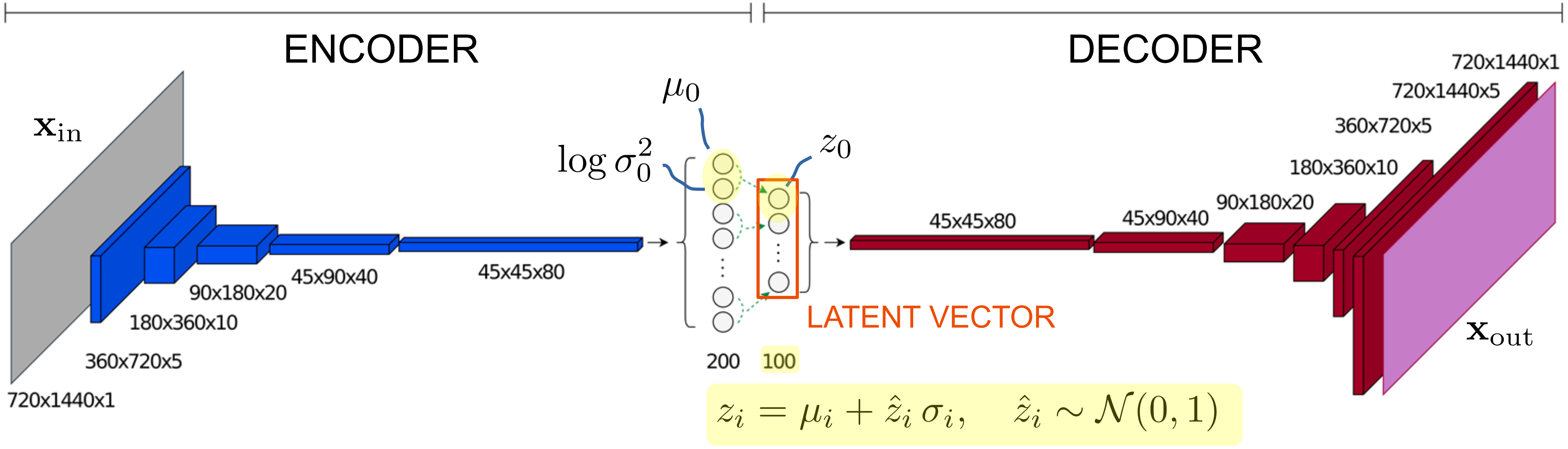

- Training: reconstruction + regularisation
- Regularisation ensures **Gaussian properties of the latent vector elements** required for variational DA, and **smoothness of the latent space**

3D-Var cost function

- Assumptions:
  - Background and observations are independent
  - Their errors are Gaussian
- Cost function:

$$\mathcal{J}(\mathbf{x}) = \mathcal{J}_b + \mathcal{J}_o =$$
$$= (\mathbf{x} - \mathbf{x}_b)^{\mathrm{T}} \mathbf{B}^{-1} (\mathbf{x} - \mathbf{x}_b) + \{\mathbf{y} - H(\mathbf{x})\}^{\mathrm{T}} \mathbf{R}^{-1} \{\mathbf{y} - H(\mathbf{x})\}$$

x ... state of the atmosphere in the grid point space
$\mathbf{x}_b$ ... background vector
B ... background-error covariance matrix
y ... observation vector
H ... observation operator
R ... observation-error covariance matrix

$$\mathbf{x}_a = \arg\min_{\mathbf{x}} \mathcal{J}(\mathbf{x})$$

$\mathbf{x}_a$ ... analysis

- Conventional cost function:

$$\mathcal{J}(\mathbf{x}) = \mathcal{J}_b + \mathcal{J}_o = \\ = (\mathbf{x} - \mathbf{x}_b)^{\mathrm{T}} \mathbf{B}^{-1} (\mathbf{x} - \mathbf{x}_b) + \{\mathbf{y} - H(\mathbf{x})\}^{\mathrm{T}} \mathbf{R}^{-1} \{\mathbf{y} - H(\mathbf{x})\}$$

- Cost function in latent space:

$$\mathcal{J}_z(\mathbf{z}) = \mathcal{J}_{bz} + \mathcal{J}_{oz} = \\ = (\mathbf{z} - \mathbf{z}_b)^{\mathrm{T}} \mathbf{B}_z^{-1} (\mathbf{z} - \mathbf{z}_b) + [\mathbf{y} - H\{D(\mathbf{z})\}]^{\mathrm{T}} \mathbf{R}^{-1} [\mathbf{y} - H\{D(\mathbf{z})\}]$$

$\mathbf{z}$ ... latent vector

$\mathbf{z}_b$ ... background defined in latent space

$\mathbf{B}_z$ ... background-error covariance matrix

$\mathbf{y}$ ... observations vector

H ... observation operator

D ... decoder

$\mathbf{R}$ ... observation-error covariance matrix

$$\mathbf{z}_a = \arg\min_{\mathbf{z}} \mathcal{J}_z(\mathbf{z})$$

$\mathbf{z}_a$ ... latent space analysis

Setup of observing system simulation experiments

- **Background simulated from ground truth for previous day** (*d-1*)
- Observations simulated from ground truth for present day (*d*)
- **Ensemble approach**: 150 ensemble members for background (perturbed according to $\mathbf{B}_z$) and observations (perturbed according to **R**)

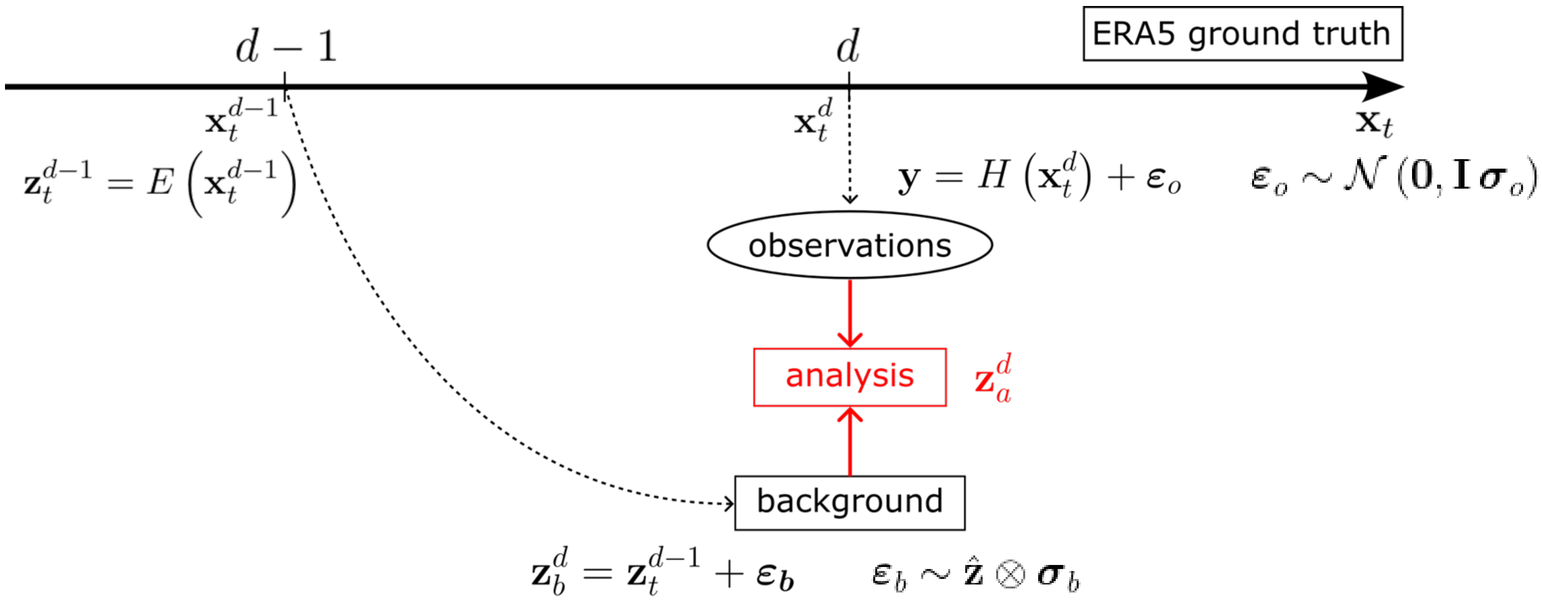

Background-error covariance matrix

$$\mathbf{B}_z = \left\langle (\mathbf{z}_b - \mathbf{z}_t)\,(\mathbf{z}_b - \mathbf{z}_t)^{\mathrm{T}} \right\rangle$$
$$= \left\langle \left(\mathbf{z}_t^{d-1} - \mathbf{z}_t^{d}\right)\,\left(\mathbf{z}_t^{d-1} - \mathbf{z}_t^{d}\right)^{\mathrm{T}} \right\rangle$$

- $\mathbf{B}_z$ quasi-diagonal => we **only use the diagonal elements** for its inverse
- Sampling perturbed background latent vectors:
  - Recall from VAE:

$$z_i = \mu_{Ei} + \hat{z}_i\,\sigma_{Ei}, \quad \hat{z}_i \sim \mathcal{N}(0,1)$$

  - What we do:

$$z_{bi} = \mu_{Ei} + \hat{z}_i\,\sigma_{bi}, \quad \hat{z}_i \sim \mathcal{N}(0,1)$$

abs($\mathbf{B}_z$), included dates 2015-01-01 to 2018-12-31

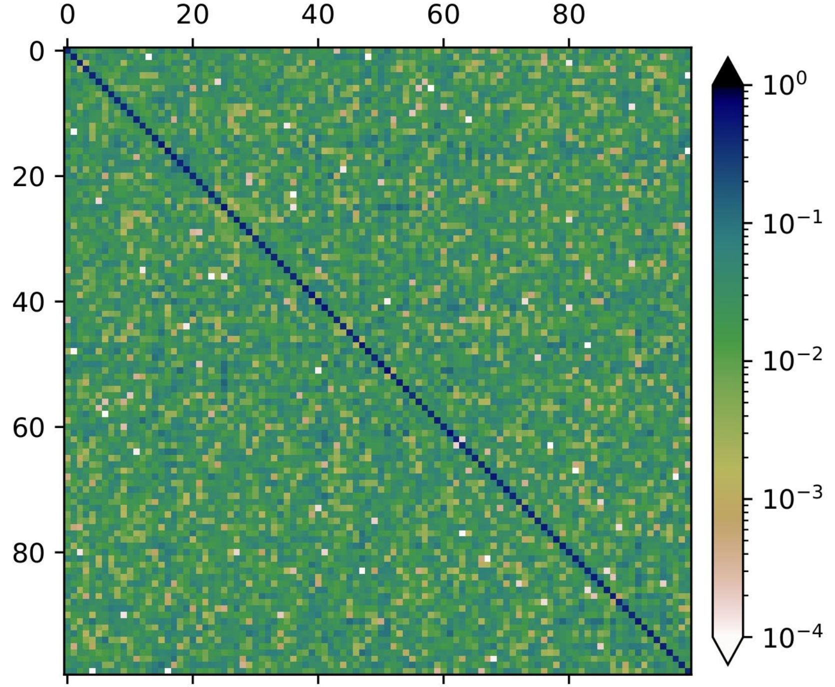

Single observation experiments in midlatitudes

- **Example:** observation above **Ljubljana, Slovenia** (46.1°N, 14.5°E)
- Background for 2019-04-15
- Preset observation departure $\delta T^o_{850} = T^o_{850} - T^b_{850} = 3\,\mathrm{K}$
  and standard deviation $\sigma_o = 1\,\mathrm{K}$

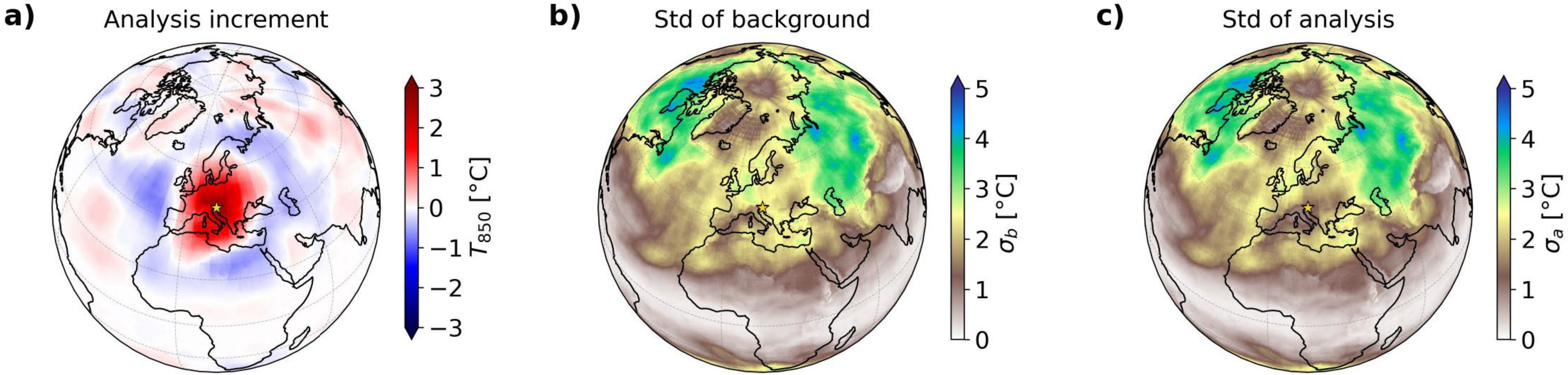

- Increment peaks at the observation location
- Increment stretched in SW-NE (typical SW winds)
- Positive increment surrounded by a shallower negative increment (spatial translation of synoptic Rossby waves typical for climatological **B** matrices (Fisher, 2003))
- Increments further away have negligible magnitude
- σ_a significantly reduced with respect to σ_b only in the area of the positive increment

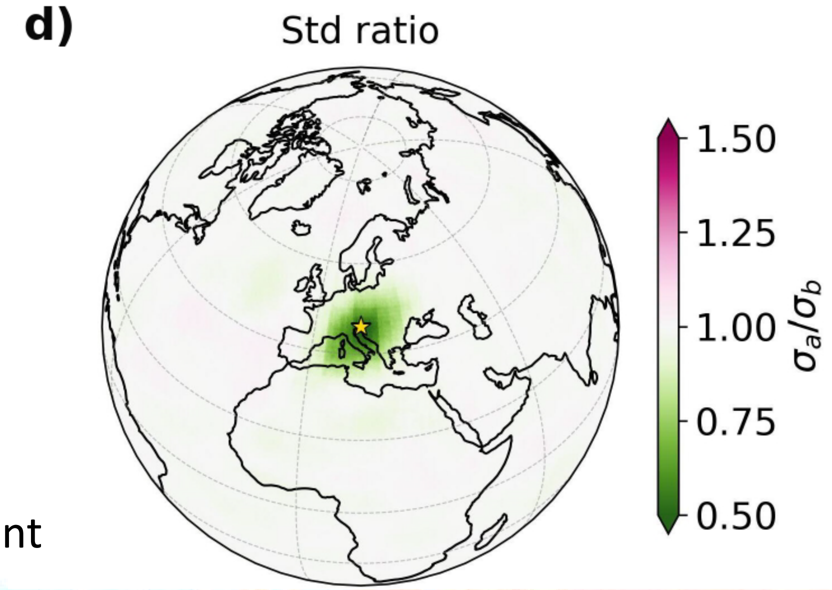

Single observation experiments in tropics

- **Example:** observation above **Eastern Equatorial Pacific** (0°N, 85°E) ($\delta T^o_{850} = 3\,\mathrm{K}, \sigma_o = 1\,\mathrm{K}$)
- ENSO pattern
- Weak increment as $\sigma_o \gg \sigma_b$
- Same magnitude of increment in tropics and midlatitudes as σ_b in the midlatitudes is much greater than in the tropics (climatological **B** matrix (Fisher, 2003))
- σ_a/σ_b reduction elongated towards W (lower branch of Pacific Walker circulation)

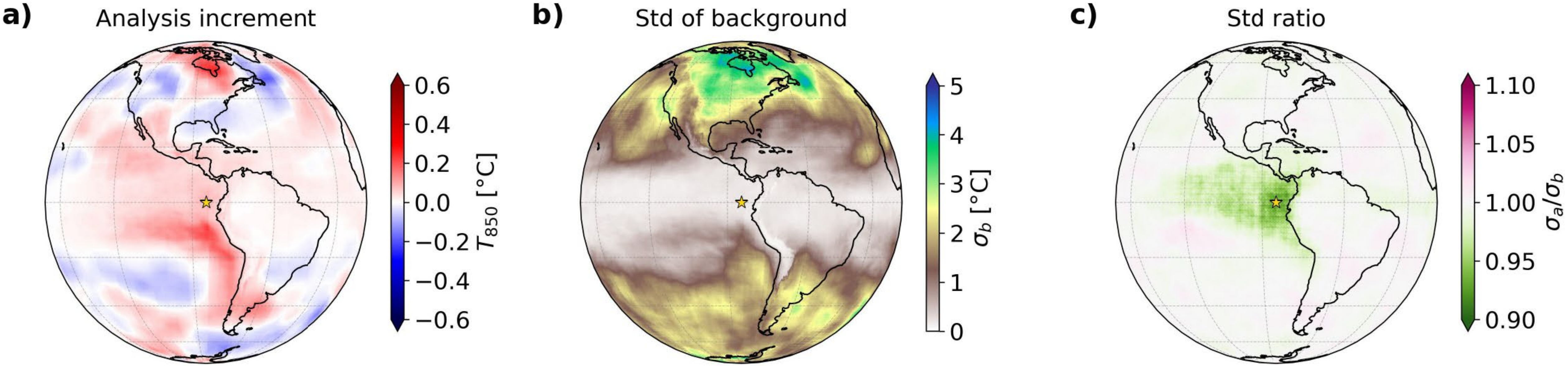

Quarterly Journal of the Royal Meteorological Society

RMetS

RESEARCH ARTICLE | Open Access

3D-Var data assimilation using a variational autoencoder

Boštjan Melinc, Žiga Zaplotnik

First published: 24 April 2024 | https://doi.org/10.1002/qj.4708

Single observation experiments: multivariate case $(Z_{200}, u_{200}, v_{200})$

- **Ljubljana**
- Observed Z_{200}

$$\delta Z^o_{200} = 300\,\mathrm{m}^2/\mathrm{s}^2$$

$$\sigma_o = 100\,\mathrm{m}^2/\mathrm{s}^2$$

- Top row:
Correlation and cross-correlation functions derived using the geostrophic increment assumption (from Kalnay, 2003)

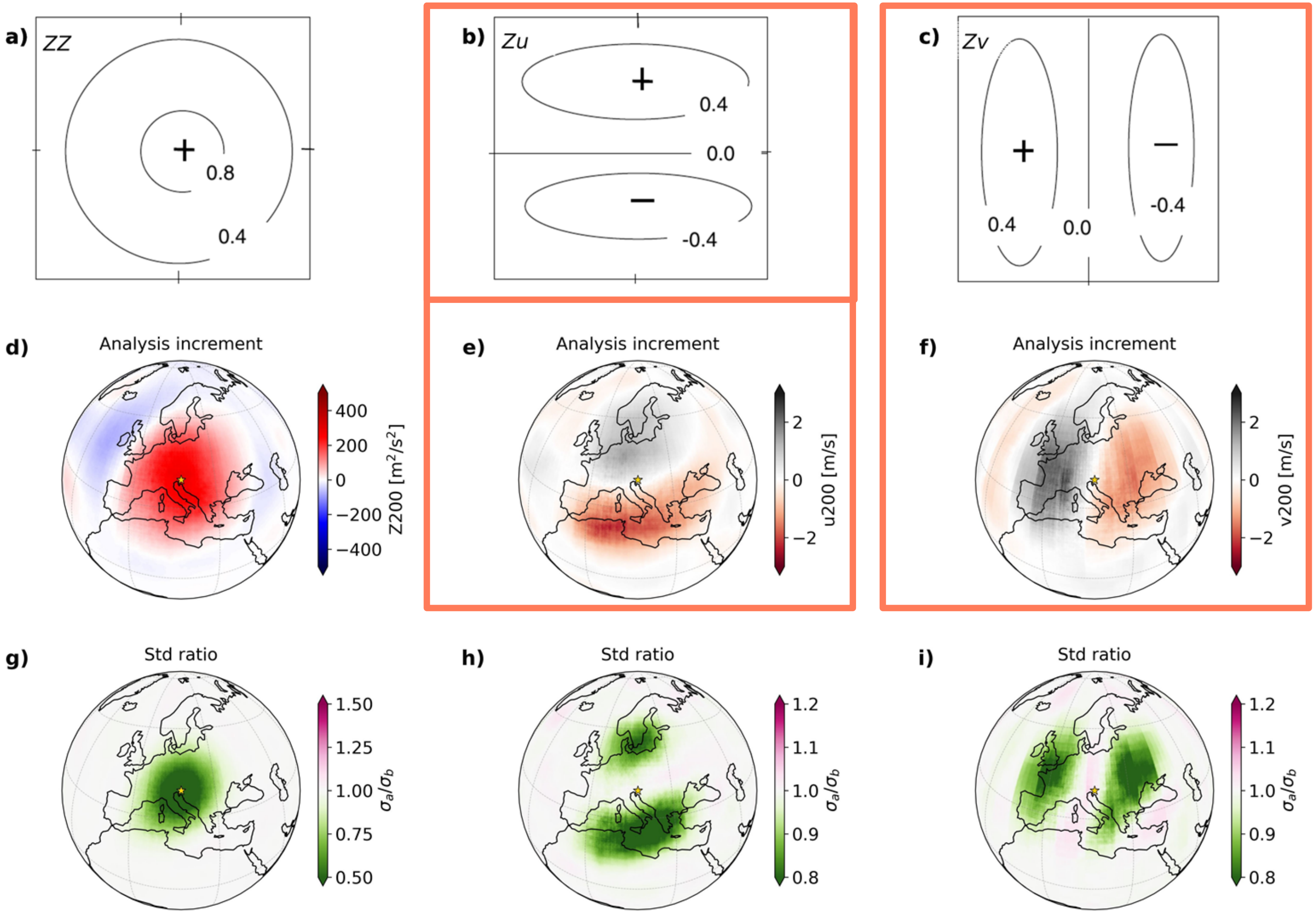

VAE alternatives

- The advantages of VAE over standard AE:
  - **Gaussian properties of the latent vector elements**
  - **Smoothness** of the latent space
- Downsides of VAE for our approach:
  - Loss function: trade-off between reconstruction and regularization
  - We do not need stochasticity
- Possible alternative: **Probabilistic AutoEncoder (PAE)** (Böhm and Seljak, 2022)
  1. Train a standard AE (reconstruction)
  2. Train a bijective transformation (normalizing flow, NF) from possibly non-Gaussian latent space ***z*** to Gaussian latent space ***u*** (regularisation)

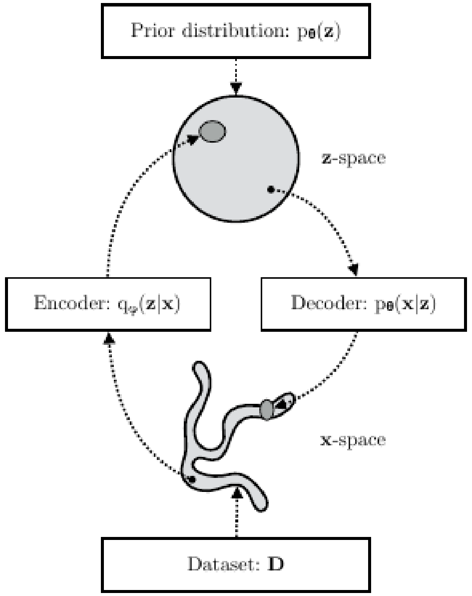

Kingma and Welling (2019)

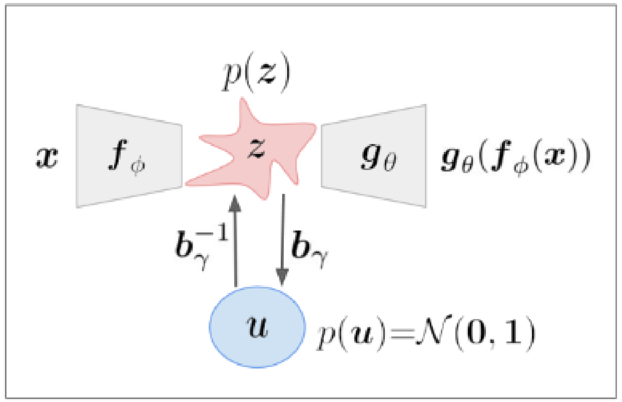

Böhm and Seljak (2022)

Probabilistic autoencoder (PAE)

- Similar structure of AE as in VAE + NF (RealNVP)

$$\mathbf{B}_u = \left\langle (\mathbf{u}_t - \mathbf{u}_b)\ (\mathbf{u}_t - \mathbf{u}_b)^{\mathrm{T}} \right\rangle$$
$$= \left\langle \left(\mathbf{u}_t^d - \mathbf{u}_t^{d-1}\right)\ \left(\mathbf{u}_t^d - \mathbf{u}_t^{d-1}\right)^T \right\rangle$$

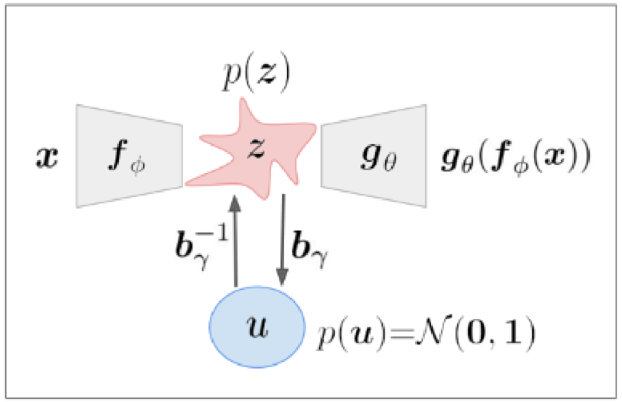

Böhm and Seljak (2022)

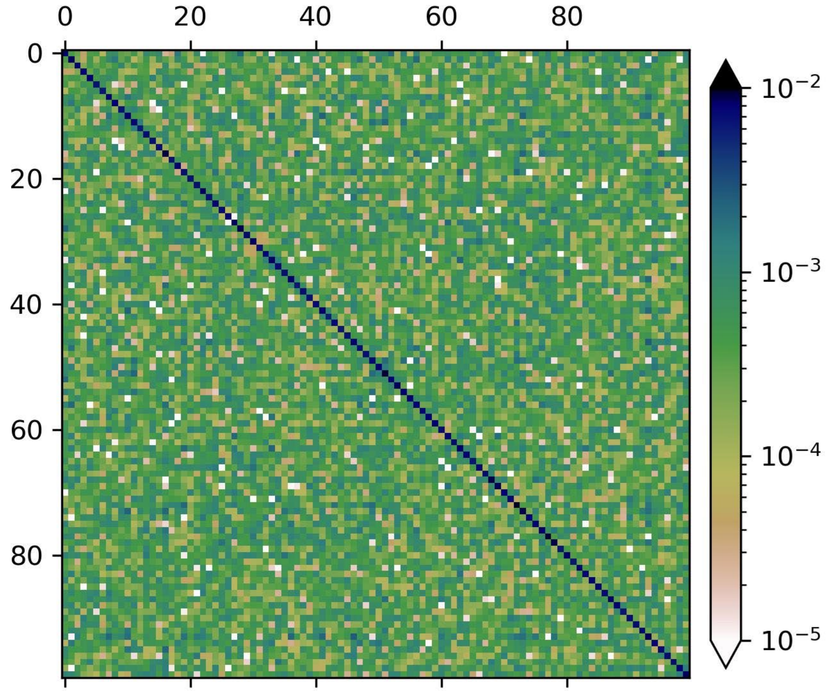

Increment comparison – Ljubljana

VAE

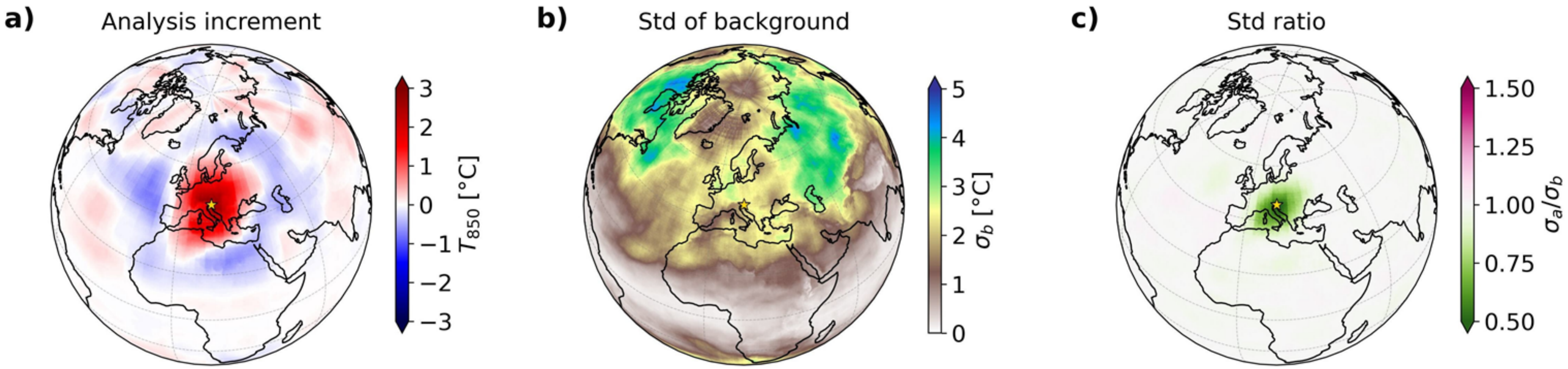

PAE

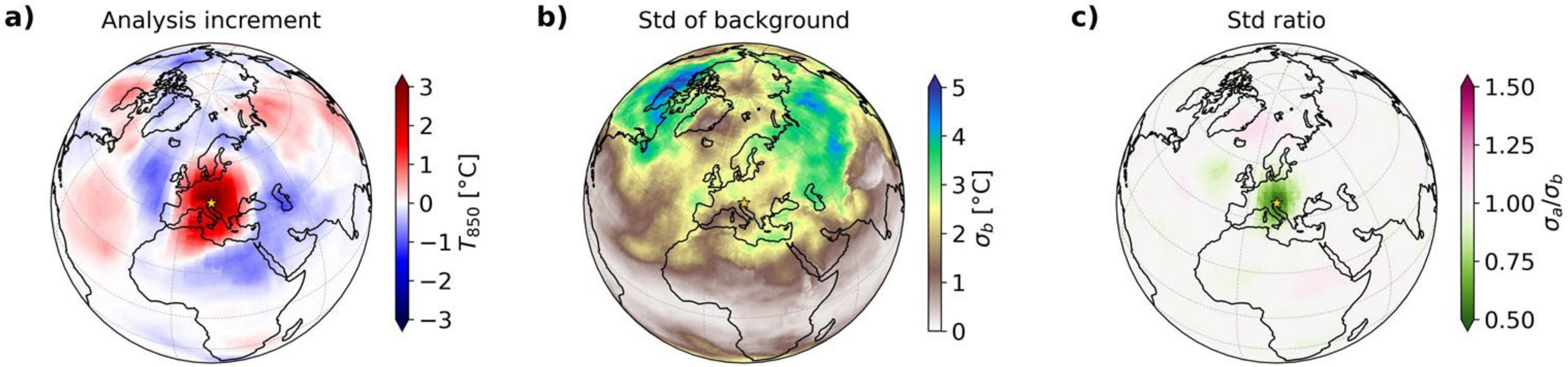

Increment comparison – Eastern Equatorial Pacific

VAE

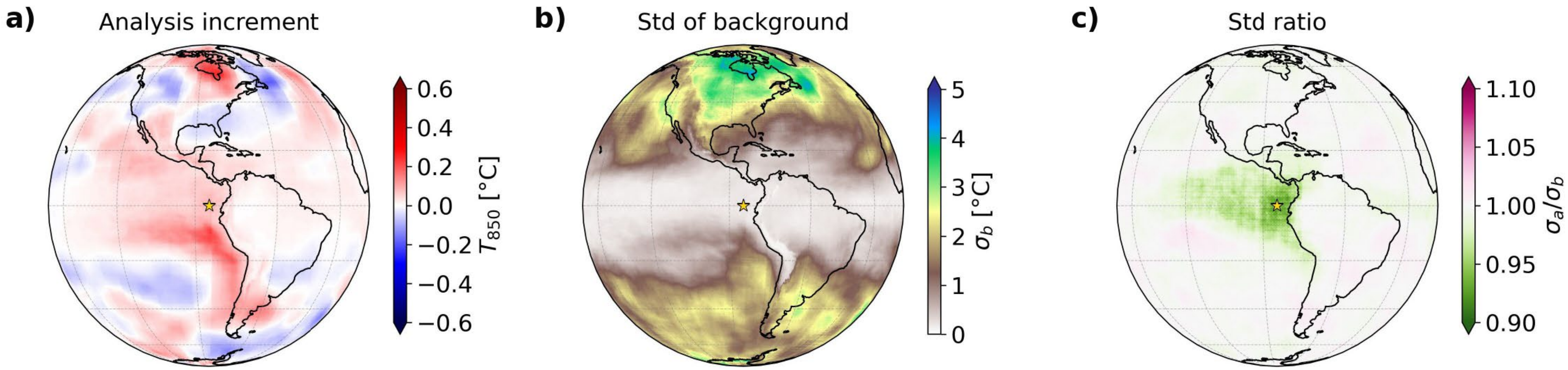

PAE

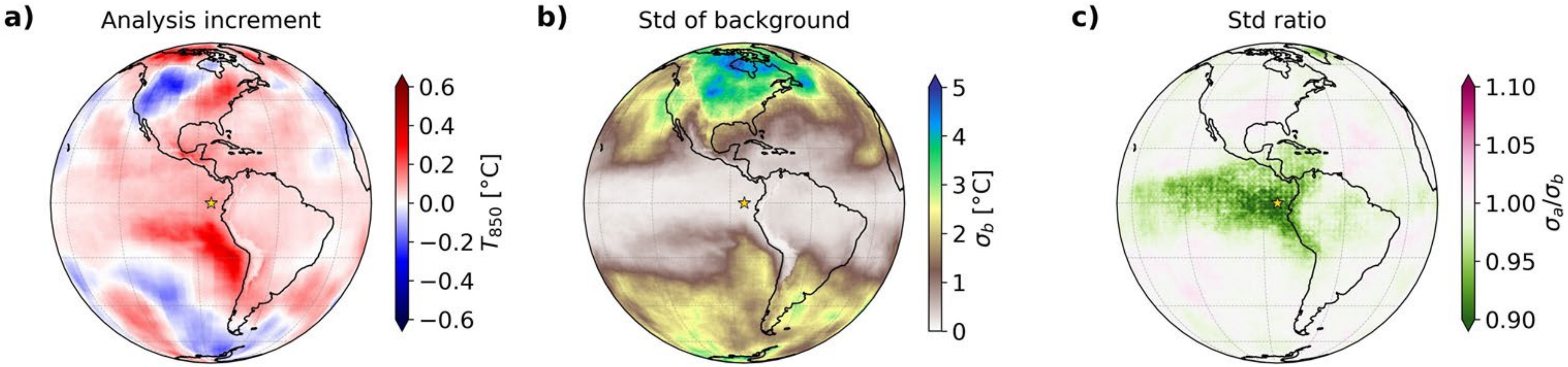

Conclusions and outlook

- We propose a neural-network-based method for variational data assimilation of atmospheric observations in a reduced-dimension latent space discovered by an autoencoder-like neural network
- We define a 3D-Var cost function in the latent space
- $\mathbf{B}_z$ is shown to be **quasi-diagonal**
- $\mathbf{B}_z$ provides a **unified representation of both tropical and extratropical covariances**
- We aim to further extend this method to:
  - multiple variables and levels,
  - 4D-Var,
  - using ensemble information to construct flow-dependent $\mathbf{B}_z$ which captures the errors associated with the current state of the atmospheric flow,
  - represent smaller-scale balances

Bibliography

- V. Böhm and U. Seljak. Probabilistic Autoencoder. 2022. URL https://arxiv.org/abs/2006.05479v4.
- P. Brohan. Machine Learning for Data Asimilation. 2022. URL https://github.com/philip-brohan/Proxy_20CR.
- M. Fisher. Background error covariance modelling. In *Seminar on Recent Development in Data Assimilation*, pages 45–63, Shinfield Park, Reading, 2003. ECMWF, ECMWF.
- A. E. Gill. Some simple solutions for heat-induced tropical circulation. *Quarterly Journal of the Royal Meteorological Society*, 106(449):3759–3777, 1980.
- B. J. Hoskins and D. J. Karoly. The steady linear response of a spherical atmosphere to thermal and orographic forcing. *Journal of the atmospheric sciences*, 38(6), 1179-1196, 1981.
- E. Kalnay. *Atmospheric Modeling, Data Assimilation and Predictability*. Cambridge Univesity Press, 2003.
- D. P. Kingma and M. Welling. An introduction to variational autoencoders. *Foundations and Trends in Machine Learning*, 12(4):307–392, 2019.
- B. Melinc and Ž. Zaplotnik. 3D-Var data assimilation using a variational autoencoder. *Quarterly Journal of the Royal Meteorological Society*, 2024. URL https://doi.org/10.1002/qj.4708.

Representation of temperature fields with VAE

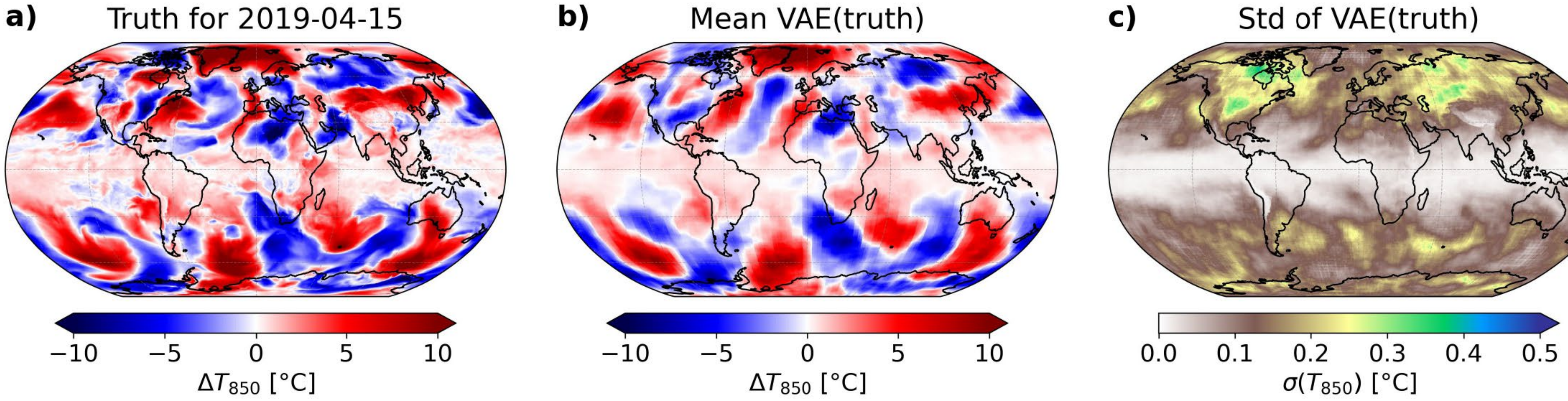

Quantitative evaluation for single observation experiments

- **Example:** observation above **Ljubljana, Slovenia** (46.1°N, 14.5°E)
- Theoretical analysis increment and standard deviation at observation location:

$$\delta T^a_{850} = \frac{\delta T^o_{850}/\sigma_o^2}{1/\sigma_b^2 + 1/\sigma_o^2} \qquad \sigma_a = \sqrt{\frac{1}{1/\sigma_b^2 + 1/\sigma_o^2}}$$

- Experimental results:

Location	$\boldsymbol{\delta T^o_{850}}$	$\boldsymbol{\sigma_o}$	$\boldsymbol{\sigma_b}$	Theo. $\boldsymbol{\delta T^a_{850}}$	Ex. $\boldsymbol{\delta T^a_{850}}$	Theo. $\boldsymbol{\sigma_a}$	Ex. $\boldsymbol{\sigma_a}$
Ljubljana	3.03	1.07	1.91	2.31	2.19	0.93	0.94
SW Indian Ocean	3.14	0.95	3.86	2.96	2.95	0.92	0.95
Singapore	3.11	0.99	0.19	0.11	0.08	0.18	0.18
Equatorial Africa	3.14	1.10	0.61	0.75	0.59	0.54	0.54
E Pacific	2.93	1.08	0.22	0.12	0.09	0.22	0.21